

Diffusion and Viscosity Equations of State for a Lennard–Jones Fluid Obtained from Molecular Dynamics Simulations

R. L. Rowley^{1,2} and M. M. Painter¹

Received February 26, 1997

Equilibrium molecular dynamics simulations were performed for a Lennard–Jones fluid at 171 conditions spanning the range $0 \leq \rho^+ \leq 1.0$ and $0.8 \leq T^+ \leq 4.0$. The Einstein or mean-squared-displacement (MSD) formula was used to compute the self-diffusion coefficient and a recently suggested, modified MSD equation was used to compute the shear viscosity at each condition. Analytical equations for the self-diffusion and viscosity coefficients were then fitted to the simulated data as polynomial functions of ρ^+ and T^+ . The resultant smoothing equations correlate the simulated data quite well and agree with argon experimental data within the uncertainty of the data.

KEY WORDS: computer simulations; diffusion; Lennard–Jones fluid; viscosity.

1. INTRODUCTION

The Lennard–Jones (LJ) potential has been widely used to study the behavior of simple fluids. Although the LJ potential is known to be simpler in functional form than most real intermolecular interactions, it nevertheless captures much of the essential physics of simple fluids. It is sufficiently accurate that it provides a convenient model for testing liquid theories and investigating fluid phenomena. Because of the importance of this model in development of theory and its ability to model the main characteristics of simple fluids, many LJ simulations have been performed and the simulated pressure–density–temperature surface has been fitted to analytical equations of state. Johnson et al. [1] cite 11 such attempts and

¹ Department of Chemical Engineering, Brigham Young University, Provo, Utah 84602, U.S.A.

² To whom correspondence should be addressed.

report a 32-parameter equation of state for the LJ fluid based on a modified Benedict–Webb–Rubin equation. Regression of this LJ equation of state included new simulations at saturation, and it therefore does a better job of correlating phase equilibrium than two previous versions [2, 3].

There have also been a significant number of simulations performed for LJ fluids in order to obtain the viscosity and self-diffusion coefficient (see, e.g., Refs. 4–7). To our knowledge, however, no general correlation of simulated diffusivities and viscosities has been reported similar to the equations of state mentioned above. One of the purposes of this study is to provide such smoothing equations that can then be used to test theories and to serve as reference equations for later development of perturbation techniques.

The second objective of this study was to test the efficacy of using a recently proposed mean-squared-displacement (MSD) method for computing viscosity. While self-diffusion coefficients have generally been obtained from simulations using the MSD algorithm, researchers have obtained viscosities exclusively using the correlation function (CF) approach. Although standard texts present both the MSD and the CF approaches as equivalent methods for obtaining transport properties from molecular simulations, viscosities obtained from MSD calculations have not been reported in the literature. While standard treatises generally do not mention any problems with the MSD approach, Erpenbeck [8] and Haile [9] both suggest that only the self-diffusion coefficient can be obtained from standard MSD formulas when periodic boundary conditions (PBC) are employed in the simulation. However, Haile proposed a modified MSD method that is compatible with PBC. This modified MSD method is tested in this study and used to obtain the values from which the final viscosity equation was regressed.

2. MOLECULAR DYNAMICS (MD) SIMULATIONS

2.1. Methodology

Standard simulation texts [10–13] describe two approaches for obtaining transport coefficients from equilibrium molecular dynamics simulations. In the CF approach, the transport coefficient is obtained from the appropriate Green–Kubo (GK) relation for the decay of correlations [10–14]. A general form of the Green–Kubo equation for a transport coefficient K can be written as

$$K = \frac{1}{G} \int_0^{\infty} \langle \dot{A}(t) \dot{A}(0) \rangle dt \quad (1)$$

Table I. EMD Variables for Calculating Pure Component Transport Coefficients

K	G	$\dot{A}(t)$	$A(t)$
D	1	$v_x(t)$	$r_x(t)$
η	kTV	$\sum_i^N \frac{p_{xi} p_{\beta i}}{m_i} + \sum_{i < j}^N r_{xi} F_{\beta i}$	$\sum_i^N p_{xi} r_{\beta i}$

where the brackets indicate the expectation value, G is a property-specific factor, A is a mechanical property of the simulation, t is time, and \dot{A} is the time derivative of A . The latter quantities are defined in Table I for the self-diffusion coefficient, D , and shear viscosity, η .

In the MSD approach, the transport coefficient is calculated from the appropriate Einstein relation that shows how the squared displacement of the appropriate variables increases in time. The general Einstein formula for a transport coefficient K can be written as

$$K = \frac{1}{2Gt} \langle [A(t) - A(0)]^2 \rangle \quad (2)$$

Helfand [14] and others [9, 13] have shown that Eq. (2) can be derived from Eq. (1) and therefore that the two methods are equivalent, at least for nonperiodic systems. Though the MSD method is commonly used to obtain self-diffusion coefficients, it has not been used for other transport properties [8]. The Einstein formulas (Helfand formalism) are still appealing because of their programming ease and the numerical accuracy obtainable from a linear least-squares fit of MSD versus time. Haile [9] recently proposed a modification of the MSD method to calculate viscosity that avoids the problems created by the periodic boundary conditions, but we know of no simulations that have used that method. We report here viscosities obtained using this new MSD algorithm and its validation.

2.2. Simulation Details

All production runs were NVT simulations performed on 256 LJ particles. The LJ potential was truncated at 4.0σ . A fifth-order predictor–corrector integration method was used with a dimensionless time step of $t^+ = 0.003$ for all but the two highest densities and temperatures; the latter conditions required a shorter time step of $t^+ = 0.001$. The runs were allowed to equilibrate for 50,000 time steps, after which information for the MSD equations was collected for the next 180,000 to 2,000,000 steps, depending upon the density and temperature.

Periodic boundary conditions were used for the mechanics of the simulation in the normal manner, but MSD calculations were based on the unfolded positions of the molecules. This was readily done by using an accumulator into which the displacement for each time step was summed before application of the periodic boundary conditions.

A multiple origin method was used to calculate MSD values in parallel. This was particularly important for η in order to improve the statistics. This can be seen from the relationships in Table I. Self diffusion is seen to be a single-particle property—a MSD value is computed for each particle. On the other hand, η is a multiparticle or system property, and a sum over all particles is required to obtain a single value of A to be used in Eq. (2). Self-diffusion computations are inherently more accurate because they include a factor of N more MSD values. Implementation of multiple time origins permits considerable improvement of the statistics for η without significant addition to the overall CPU time. This was done by overlapping or nesting the initiation of MSD calculations such that many MSD values were computed in parallel. To gain maximum statistical advantage, the parallel MSD calculations were generally separated by enough time steps that consecutive time origins were independent. At the lowest densities, where it takes several thousand time steps for the correlations to die out, initiation of the MSDs was made before loss of complete correlation in order to keep the total length of the simulation tractable. This did not cause any noticeable deterioration in the statistics of the computed transport coefficients. Specifications on the duration and spacing of various parts of the simulations are shown in Fig. 1, which is keyed to Table II.

Additional statistical accuracy was achieved by computing MSD values for each appropriate Cartesian coordinate and including these values in the averages. This gives an additional factor of three for D , while

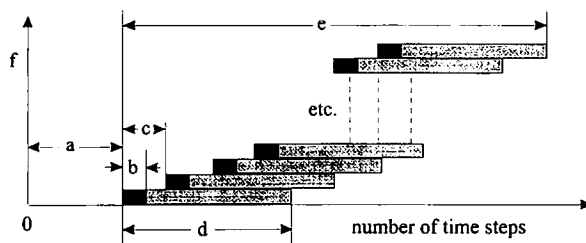


Fig. 1. Typical parts of the EMD simulation including equilibration (a), Knudsen truncation (b), separation of MSD time origins (c), length of MSD data accumulation (d), total simulation length (e), and number of time origins (f).

Table II. Number of Time Steps (in Thousands) Used for Each Part of the Simulations

T^+	ρ^+	a''	b''	c''	d''	e''	f''
0.80-1.25	0.05-0.10	50	14	1.0	22	2021	2
	0.15-0.30	50	1.0	0.5	3.5	1003	2
	0.40-0.50	50	0.25	0.25	2.25	502	2
	0.60-0.70	50	0.20	0.20	2.2	402	2
	0.80-1.0	50	0.06	0.06	2.0	182	3
1.30-4.00	0.05	50	14	1.0	8	2021	2
	0.10-0.15	50	1	0.5	2.5	1003	2
	0.20	50	0.25	0.25	2	502	2
	0.30-0.50	50	0.20	0.20	2	402	2
	0.60-1.00	50	0.06	0.06	2	182	3

'' See Fig. 1 for a key to the letters denoting parts of the simulation.

for η it yields an extra factor of six. Thus, the actual implementation of the Einstein equations of Table I into the code was done in accordance with

$$D = \frac{1}{6t} \sum_{\alpha=1}^3 \langle [r_{\alpha i}(t) - r_{\alpha i}(0)]^2 \rangle \tag{3}$$

$$\eta = \frac{1}{12VkTt} \sum_{\alpha=1}^3 \sum_{\beta=1}^3 \left\langle \left[\sum_{i=1}^N (p_{\alpha i}(t) r_{\beta i}(t) - p_{\alpha i}(0) r_{\beta i}(0)) \right]^2 \right\rangle \tag{4}$$

($\alpha \neq \beta$)

where r_x and r_β represent any of the three Cartesian coordinates, k is Boltzmann's constant, p_x represents the α component of the momentum vector, V is volume, and subscript i refers to molecule i .

Computation of the transport coefficients was done using a least-squares fit of MSD versus t in accordance with Eqs. (3) and (4). However, data at very short times were not included where the displacement is due mainly to the free-flight or Knudsen diffusion of the particles. The number of time steps excluded for this reason depended upon the density and temperature used in the simulation, but it is also reported in Table II.

2.3. Modification of the Einstein Method for Viscosity

Haile [9] and Erpenbeck [8] have shown that the Green-Kubo and Einstein equations for viscosity are not equivalent for periodic systems even with unfolded boundary conditions. Haile shows that η can, however, be

evaluated indirectly using the Einstein method. The equality of Eqs. (1) and (2) requires that the MSD can be obtained from

$$MSD = \langle [A(t) - A(0)]^2 \rangle = \int_0^\infty \langle \dot{A}(t) \dot{A}(0) \rangle dt \tag{5}$$

where the appropriate quantities for A and its time derivative are given in Table I. This method was implemented in this study by computing

$$\dot{A} = \sum_i^N \frac{p_{\alpha i} p_{\beta i}}{m_i} + \sum_i^N F_{\alpha i} r_{\beta i} \quad (\alpha \neq \beta) \tag{6}$$

where F is force, at each time step and then by using Simpson's rule to integrate numerically $\int_0^\tau \dot{A}(t) \cdot \dot{A}(0) dt$ to obtain indirectly the shear MSD at time τ . The MSD calculated in this fashion was then treated the same as that for D ; i.e., the final value of η was determined from the slope of the MSD versus time curve.

2.4. Benchmarks

Validity of the code was checked by performing benchmark studies. The results are shown in Fig. 2 as a function of dimensionless number density, ρ^+ . Agreement with literature values was generally within $\pm 6\%$

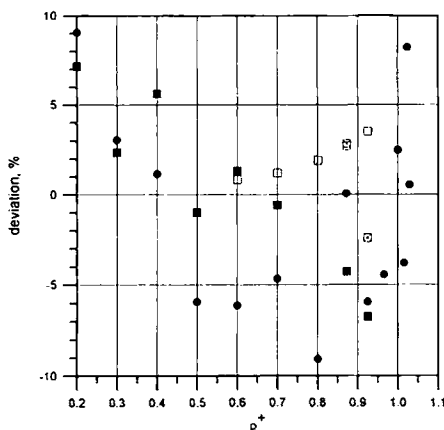


Fig. 2. Benchmark studies at $T^+ = 1.863$ showing percentage deviation of literature values [5] from the values simulated in this work for D (●) and η . (◻) Ar data; (■) CF approach from EMD; (◻) nonequilibrium molecular dynamics simulations.

with no noticeable bias. All results are given in terms of variables made dimensionless (superscript +) using the LJ parameters, ϵ and σ , and the molecular mass, m ; namely,

$$\begin{aligned}
 T^+ &= \frac{kT}{\epsilon}, & P^+ &= \frac{P\sigma^3}{\epsilon}, & \rho^+ &= \rho\sigma^3 = \frac{N}{V}\sigma^3 \\
 D^+ &= D\sqrt{\frac{\epsilon}{m\sigma^2}}, & \eta^+ &= \eta\frac{\sigma^2}{\sqrt{m\epsilon}}
 \end{aligned}
 \tag{8}$$

2.5. Simulation Results

The simulations were run at regular grid points in the ρT plane that spanned the domain $0.05 \leq \rho^+ \leq 1.00$ and $0.80 \leq T^+ \leq 4.00$. Figure 3 shows the location of the simulation points relative to the LJ phase dome calculated from the most recent LJ equation of state [1]. Simulations were performed in the two-phase region only to provide continuity of states between vapor and liquid densities in anticipation of correlating the data into polynomial equations. Values in the two-phase region have no other significance. Results for D and η at each of the 171 state points are reported in Tables III and IV. The value in boldface type is the average value of the transport coefficient obtained by averaging over all of the multiple time origins. Standard deviations, estimated from block averages over each

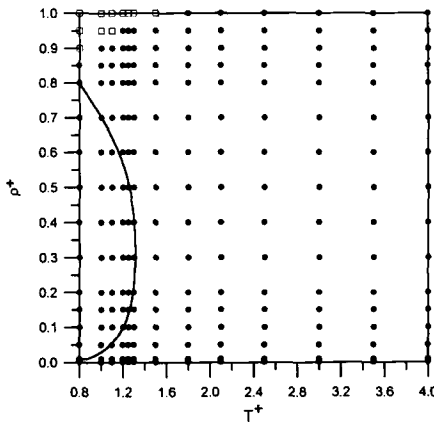


Fig. 3. Conditions relative to the LJ phase dome at which simulations were performed. Simulations were not performed at points marked with an open square because they lie in the solid region.

Table III. Simulation Results^a for D^+

ρ^+	0.80	1.00	1.10	1.20	1.25	1.30	1.50	1.80	2.10	2.50	3.00	3.50	4.00
0.05	1.747 0.007	2.769 0.029	3.093 0.004	3.421 0.007	3.527 0.016	3.694 0.039	4.292 0.003	4.959 0.009	5.573 0.066	6.525 0.077	7.620 0.086	8.562 0.018	9.239 0.006
0.10	0.624 0.004	1.337 0.025	1.530 0.007	1.681 0.010	1.759 0.002	1.798 0.007	2.049 0.003	2.412 0.000	2.759 0.002	3.175 0.010	3.646 0.013	4.081 0.012	4.510 0.027
0.15	0.355 0.007	0.813 0.008	0.984 0.010	1.105 0.006	1.147 0.003	1.196 0.008	1.379 0.002	1.613 0.006	1.824 0.007	2.081 0.006	2.386 0.013	2.667 0.018	2.918 0.005
0.20	0.259 0.003	0.579 0.004	0.720 0.003	0.816 0.005	0.860 0.001	0.857 0.002	0.988 0.001	1.149 0.003	1.298 0.003	1.492 0.001	1.708 0.001	1.919 0.004	2.115 0.008
0.30	0.173 0.001	0.378 0.000	0.468 0.003	0.526 0.001	0.550 0.003	0.555 0.004	0.636 0.003	0.733 0.010	0.828 0.005	0.941 0.006	1.077 0.011	1.207 0.008	1.317 0.011
0.40	0.143 0.002	0.281 0.003	0.330 0.003	0.363 0.004	0.380 0.001	0.392 0.002	0.444 0.003	0.514 0.003	0.577 0.003	0.654 0.004	0.752 0.006	0.835 0.006	0.923 0.006
0.50	0.135 0.001	0.216 0.003	0.241 0.002	0.264 0.001	0.273 0.002	0.282 0.003	0.318 0.003	0.367 0.004	0.412 0.003	0.474 0.004	0.541 0.004	0.610 0.003	0.681 0.008
0.60	0.121 0.002	0.157 0.001	0.172 0.002	0.186 0.002	0.191 0.002	0.198 0.002	0.224 0.003	0.264 0.003	0.300 0.001	0.349 0.006	0.404 0.005	0.453 0.008	0.503 0.003
0.70	0.082 0.001	0.105 0.001	0.116 0.001	0.125 0.002	0.132 0.001	0.137 0.002	0.156 0.001	0.187 0.003	0.217 0.003	0.249 0.004	0.296 0.004	0.341 0.004	0.380 0.009
0.80	0.048 0.001	0.065 0.001	0.072 0.002	0.079 0.001	0.084 0.001	0.088 0.001	0.103 0.001	0.125 0.002	0.148 0.001	0.178 0.002	0.214 0.003	0.248 0.002	0.283 0.005
0.85	0.035 0.000	0.047 0.001	0.055 0.001	0.061 0.001	0.064 0.001	0.068 0.001	0.081 0.001	0.102 0.001	0.121 0.001	0.148 0.001	0.179 0.003	0.210 0.001	0.241 0.002
0.90	Solid	0.034 0.000	0.040 0.001	0.046 0.001	0.048 0.001	0.051 0.001	0.063 0.001	0.079 0.001	0.097 0.002	0.119 0.002	0.149 0.002	0.177 0.003	0.201 0.001
0.95	Solid	Solid	Solid	0.032 0.000	0.034 0.000	0.037 0.001	0.046 0.001	0.060 0.001	0.077 0.001	0.097 0.002	0.122 0.002	0.147 0.001	0.170 0.002
1.00	Solid	Solid	Solid	Solid	Solid	Solid	Solid	0.046 0.001	0.059 0.001	0.077 0.001	0.099 0.001	0.121 0.001	0.142 0.002

^aThe boldface number on top is the average value for D^+ ; the number underneath is the standard deviation based on 1000 MSD block averages. The upper boxed region represents the liquid-vapor, two-phase region; lower boxed region represents the solid.

Table IV. Simulation Results^a for η^*

ρ^*	T^*												
	0.80	1.00	1.10	1.20	1.25	1.30	1.50	1.80	2.10	2.50	3.00	3.50	4.00
0.05	0.059 0.006	0.100 0.003	0.129 0.025	0.133 0.003	0.150 0.017	0.136 0.013	0.172 0.015	0.175 0.008	0.209 0.017	0.242 0.001	0.274 0.009	0.364 0.073	0.356 0.016
0.10	0.055 0.005	0.119 0.000	0.127 0.003	0.143 0.017	0.158 0.019	0.142 0.002	0.180 0.003	0.204 0.002	0.226 0.021	0.251 0.015	0.301 0.007	0.319 0.033	0.352 0.017
0.15	0.068 0.001	0.122 0.000	0.142 0.009	0.165 0.000	0.153 0.001	0.164 0.002	0.193 0.024	0.229 0.032	0.254 0.013	0.282 0.018	0.327 0.017	0.361 0.021	0.381 0.038
0.20	0.087 0.006	0.144 0.005	0.177 0.001	0.190 0.009	0.195 0.002	0.198 0.003	0.227 0.000	0.262 0.011	0.275 0.021	0.309 0.002	0.376 0.004	0.391 0.027	0.429 0.017
0.30	0.187 0.004	0.232 0.004	0.257 0.037	0.259 0.002	0.249 0.020	0.277 0.030	0.294 0.042	0.317 0.036	0.386 0.049	0.400 0.028	0.446 0.046	0.479 0.063	0.493 0.082
0.40	0.290 0.028	0.346 0.039	0.352 0.017	0.400 0.073	0.412 0.035	0.390 0.042	0.412 0.052	0.460 0.102	0.480 0.111	0.487 0.031	0.537 0.064	0.544 0.057	0.647 0.068
0.50	0.536 0.055	0.534 0.069	0.515 0.016	0.539 0.047	0.564 0.034	0.606 0.054	0.564 0.042	0.599 0.075	0.719 0.068	0.694 0.069	0.653 0.014	0.753 0.051	0.720 0.069
0.60	0.833 0.053	0.785 0.058	0.760 0.105	0.756 0.073	0.791 0.126	0.861 0.064	0.823 0.059	0.901 0.155	0.873 0.141	0.934 0.143	1.052 0.107	0.998 0.164	1.131 0.099
0.70	1.205 0.130	1.142 0.087	1.187 0.122	1.304 0.200	1.167 0.063	1.232 0.121	1.173 0.032	1.184 0.108	1.341 0.030	1.213 0.138	1.390 0.041	1.423 0.201	1.564 0.145
0.80	2.325 0.410	1.943 0.183	2.079 0.164	2.291 0.277	2.029 0.321	1.934 0.192	1.924 0.322	1.941 0.234	1.852 0.455	1.826 0.241	1.757 0.178	1.919 0.108	1.894 0.119
0.85	3.492 0.261	3.019 0.223	2.593 0.353	2.415 0.219	2.547 0.313	2.674 0.438	2.332 0.210	2.223 0.091	2.500 0.413	2.337 0.238	2.151 0.308	2.224 0.255	2.165 0.366
0.90	Solid Solid	4.060 0.827	4.011 0.546	3.321 0.496	3.306 0.419	3.313 0.386	3.295 0.570	3.104 0.349	3.248 0.466	2.890 0.282	2.933 0.224	2.504 0.353	2.756 0.353
0.95	Solid	Solid	5.588 0.766	5.167 0.574	4.524 0.591	4.566 0.196	3.797 0.359	3.578 0.514	3.578 0.484	3.532 0.865	3.116 0.376	3.601 0.484	2.940 0.457
1.00	Solid	Solid	Solid	Solid	Solid	Solid	Solid	5.374 0.323	5.179 0.994	4.282 0.519	4.290 0.308	4.279 0.716	3.850 0.330

^aThe boldface number on top is the average value for η^* ; the number underneath is the standard deviation based on 1000 MSD block averages. The upper boxed region represents the liquid-vapor, two-phase region; the lower boxed region represents the solid.

1000 time origins, are reported in this table directly below the average value in normal type.

3. LJ TRANSPORT EQUATIONS

The simulation results, combined with Chapman-Enskog values at $\rho = 0$, were used to regress coefficients in equations of the form

$$K = K_0 + \sum_{i=1}^6 \sum_{j=1}^6 \frac{b_{ji}}{(T^+)^{(j-1)}} (\rho^+)^i \quad (8)$$

where K is $\rho^+ D^+$ for self diffusion and $\ln \eta^+$ for shear viscosity; K_0 is the Chapman-Enskog low-density value. We have also correlated the Chapman-Enskog collision integrals as a function of temperature so that the final equations may be written simply as

$$D^+ = \frac{1}{\rho^+} \left[\rho^+ D_0^+ + \sum_{i=1}^4 \sum_{j=1}^6 b_{ji} \frac{(\rho^+)^i}{(T^+)^{(j-1)}} \right]$$

$$\rho^+ D_0^+ = \frac{3}{8} \sqrt{\frac{T^+}{\pi}} \left(\sum_{i=1}^6 \omega_i (T^+)^{j-1} \right)^{-1} \quad (9)$$

$$\eta^+ = \eta_0^+ \exp \left[\sum_{i=1}^4 \sum_{j=1}^6 b_{ji} \frac{(\rho^+)^i}{(T^+)^{(j-1)}} \right]$$

$$\eta_0^+ = \frac{5}{16} \sqrt{\frac{T^+}{\pi}} \left(\sum_{j=1}^5 \omega_j (T^+)^{j-1} \right)^{-1} \quad (10)$$

Table V. Constants for Use in the Transport Equations

Property	j	b_{j1}	b_{j2}	b_{j3}	b_{j4}	ω_j
D_+	1	-2.19672	6.86168	-9.18961	3.8867	3.3667
	2	15.6693	-59.1879	78.9642	-33.6443	-3.7718
	3	-48.8200	200.229	-272.009	117.554	2.6692
	4	75.3823	-321.603	441.017	-192.079	-0.9953
	5	-55.5212	242.752	-335.146	146.837	0.1863
	6	15.1673	-67.8152	94.3826	-41.6192	-0.0138
η^+	1	-7.53814	36.0319	-47.0432	19.7791	2.8745
	2	66.0342	-299.373	430.291	-191.670	-2.2065
	3	-220.881	10.6797	-1575.25	725.006	0.9158
	4	334.883	-1638.92	2445.08	-1140.09	-0.1960
	5	-226.756	1112.30	-1669.43	783.084	0.0160
	6	52.4394	-255.199	380.704	-176.589	—

where the coefficients b_{ji} and ω_j for each property are tabulated in Table V. These transport equations adequately represent the simulated data over the domain $0 \leq \rho^+ \leq 1.0$ and $0.8 \leq T^+ \leq 4.0$. The average absolute deviation (AAD) between the simulated D values and those correlated by Eq. (10) was 3.14% (2.06% excluding points in the two-phase region) and the bias was +1.85% (+0.48% excluding points in the two-phase region). For viscosity, the AAD was 4.34% (4.40% excluding two-phase points) with a bias of -0.47% (-0.30% excluding two-phase points).

4. EFFECTIVENESS OF THE DEVELOPED TRANSPORT EQUATIONS

As mentioned, the regressed transport equations should be valid over the domain bounded by $0 \leq \rho^+ \leq 1.0$ and $0.8 \leq T^+ \leq 4.0$; they should not be used outside that range. The average absolute deviations mentioned above are probably a reasonable estimate of the uncertainties inherent in the equations; about 3% for diffusion and about 4.5% for viscosity.

We thought it also informative to compare values calculated from the various LJ equations with correlations of experimental argon data

Table VI. Percentage Deviation of η , Calculated from Eq. (10), from a Correlation of Argon Viscosities^a [15, 16]

T (K)	P (bar)							
	1	20	40	100	200	400	600	1000
120	-1.51 (0.0024)	0.18 (0.7021)	-2.07 (0.7114)	-3.51 (0.7344)	-2.95 (0.7630)	0.83 (0.8037)	— (0.8433)	— (0.8738)
150	-0.65 (0.0019)	-6.60 (0.0457)	-5.04 (0.1264)	2.62 (0.5800)	3.21 (0.6499)	3.12 (0.7187)	3.56 (0.7613)	4.37 (0.8193)
200	0.25 (0.0015)	-3.56 (0.0307)	-6.68 (0.0657)	-6.31 (0.2032)	-0.82 (0.4210)	6.31 (0.5759)	7.69 (0.6464)	7.63 (0.7288)
250	0.05 (0.0012)	-2.55 (0.0238)	-4.77 (0.0487)	-8.56 (0.1303)	-7.61 (0.2694)	1.45 (0.4509)	5.80 (0.5447)	9.03 (0.6494)
300	-0.31 (0.0010)	-2.38 (0.0195)	-4.15 (0.0394)	-7.32 (0.1009)	-7.55 (0.2023)	-1.01 (0.3622)	1.60 (0.4618)	6.85 (0.5805)
350	-1.24 (0.0008)	-2.82 (0.0166)	-4.06 (0.0333)	-6.53 (0.0837)	-7.78 (0.1650)	-4.42 (0.3013)	-0.39 (0.3983)	4.32 (0.5226)
400	-1.46 (0.0007)	-2.82 (0.0145)	-3.88 (0.0289)	-6.06 (0.0719)	-7.45 (0.1407)	-5.73 (0.2592)	-2.49 (0.3503)	2.63 (0.4736)
450	-1.59 (0.0006)	-2.80 (0.0128)	-3.80 (0.0256)	-5.93 (0.0633)	-7.42 (0.1233)	-6.55 (0.2283)	-3.92 (0.3133)	1.44 (0.4334)

^a The lower entry is the reduced density corresponding to the given T and P .

available in the literature. The LJ parameters used for this comparison were $\sigma = 3.418 \text{ \AA}$ and $\varepsilon/k = 124.0 \text{ K}$ [11]. Table VI shows the percentage deviations of the viscosity equation obtained over a range of densities and temperatures from correlated argon data [15, 16]. The overall AAD and bias at the compared conditions were 5.3 and -2.2% , respectively. While this is within the combined uncertainties of the experimental correlation (about 4%) and the transport equation (4.5%), we do not imply that Ar is a LJ fluid. Argon densities actually deviate from the LJ equation of state by about 2% in the liquid region, but the comparison does provide an independent check on the validity of the new MSD computations.

5. CONCLUSIONS

EMD simulations of the LJ fluid were performed at 171 state points from which self-diffusion and shear viscosity coefficients were computed using the MSD or Einstein relations. These simulated values were used to obtain smoothing equations for the LJ fluid as a function of temperature and density over the range $0 \leq \rho^+ \leq 1.0$ and $0.8 \leq T^+ \leq 4.0$. The newly developed LJ transport equations correlated the simulated values adequately and represent Ar experimental data quite well. We conclude that the modified Einstein method suggested by Haile [9] is a viable means for obtaining accurate viscosity values. Finally, we should mention that thermal conductivity and bulk viscosity can also be calculated from Haile's modified Einstein approach.

ACKNOWLEDGMENT

Acknowledgment is made of the donors of The Petroleum Research Fund, administered by the ACS, for partial support of this research.

REFERENCES

1. J. K. Johnson, J. A. Zollweg, and K. E. Gubbins, *Mol. Phys.* **78**:591 (1993).
2. Y. Adachi, I. Fijihara, M. Takamiya, and K. Nakanishi, *Fluid Phase Equil.* **39**:1 (1988).
3. J. J. Nicolas, K. E. Gubbins, W. B. Streett, and D. J. Tildesley, *Mol. Phys.* **37**:1429 (1979).
4. D. M. Heyes, *Phys. Rev. B* **37**:5677 (1988).
5. R. Castillo, A. Villaverde, and J. Orozco, *Mol. Phys.* **74**:1315 (1991).
6. K. D. Hammonds and D. M. Heyes, *J. Chem. Soc. Faraday Trans. 2* **84**:705 (1988).
7. D. M. Heyes, *J. Chem. Soc. Faraday Trans. 2* **79**:1741 (1983).
8. J. J. Erpenbeck, *Phys. Rev. E* **51**:4296 (1995).
9. J. M. Haile, *Molecular Dynamics Simulation* (Wiley, New York, 1992).
10. M. P. Allen and D. J. Tildesley, *Computer Simulation of Liquids* (Clarendon Press, Oxford, 1987).

11. R. L. Rowley, *Statistical Mechanics for Thermophysical Property Calculations* (Prentice-Hall, Englewood Cliffs, NJ, 1994).
12. J. P. Hansen and I. R. McDonald, *Theory of Simple Liquids*, 2nd ed. (Academic Press, San Diego, 1986).
13. W. A. Steele, *Time-Correlation Functions*, in H. J. M. Hanley, ed., *Transport Phenomena in Fluids* (Marcel Dekker, New York, 1969), p. 209.
14. E. Helfand, *Phys. Rev.* **119**:1 (1960).
15. V. A. Rabinovich, A. A. Vasserman, V. I. Nedostup, L. S. Veksler, and T. B. Selover, Jr. (English edition editor), *Thermophysical Properties of Neon, Argon, Krypton, and Xenon* (Hemisphere, Washington, DC, 1988).
16. N. B. Vargaftik, *Handbook of Physical Properties of Liquids and Gases*, 2nd ed. (Hemisphere, Washington, DC, 1975).